Metal-Semiconductor Nanocontacts: Silicon Nanowires

Uzi Landman,[1] Robert N. Barnett,[1] Andrew G. Scherbakov,[1] and Phaedon Avouris[2]
[1]*School of Physics, Georgia Institute of Technology, Atlanta, Georgia 30332-0430*
[2]*IBM Research Division, T. J. Watson Research Center, Yorktown Heights, New York 10598*
(Received 16 November 1999)

Silicon nanowires assembled from clusters or etched from the bulk, connected to aluminum electrodes and passivated, are studied with large-scale local-density-functional simulations. Short (~0.6 nm) wires are fully metallized by metal-induced gap states resulting in finite conductance ($\sim e^2/h$). For longer wires (~2.5 nm) nanoscale Schottky barriers develop with heights larger than the corresponding bulk value by 40% to 90%. Electric transport requires doping dependent gate voltages with the conductance spectra exhibiting interference resonances due to scattering of ballistic channels by the contacts.

PACS numbers: 73.40.Sx, 73.40.Cg, 73.20.Dx

As the relentless miniaturization of electronic devices is reaching the nanometer scale, current device concepts may have to be radically modified due to the nonscalable nature of materials in this size range, with an emphasis on quantum mechanical effects [1]. However, while of significant fundamental interest and of high technological relevance, answers to such issues, in the form of reliable estimates of properties calculated and/or measured for nanoscale materials structures, pertaining to characteristics of individual nanoscale device components and their interconnections, are largely unavailable.

We report on large-scale *ab initio* simulations [2], providing first insight into the structures, electronic spectra, and transport properties of surface-passivated silicon nanowires (SiNWs) [3], etched from bulk Si or prepared via a novel cluster assembly, and their contacts to aluminum electrodes. For a very short (~0.6 nm) SiNW bridging the Al electrodes we find full metallization by metal-induced-gap states (MIGS) resulting in a finite electronic conductance ($\sim e^2/h$), while for longer wires (~2.5 nm) highly localized interfacial dipoles form which together with pinning of E_F at the neutrality level result in nanoscale Schottky barriers with heights larger than the barrier at the corresponding bulk interface by 40% to 90%, depending on the type of SiNW and the interfacial atomic structure. Transport through the longer wires requires doping dependent gate voltages and the conductance spectra exhibit size-dependent oscillations due to interference resonances, originating from scattering of the ballistic conductance eigenchannels from the contacts.

In constructing the SiNWs we considered two strategies: (1) assembly of wires from silicon clusters [4], i.e., formation of cluster-derived (CD) SiNWs; see Fig. 1 where shown in (ii) is a Si_{24} cluster bridging the two Al electrodes, referred to as Si_{24}NW, and displayed in (iii) is a wire made of five base-sharing Si_{24} clusters attached to the Al electrodes, referred to as Si_{96}NW, and (2) etching of wires out of bulk Si; see Fig. 1(i) where shown is an electrode-attached diamond-structured (DS) wire with its long axis along the [211] direction and exposing $(1\bar{1}\bar{1})$ and $(01\bar{1})$ surfaces [3a,3d], referred to as Si_{94}NW [5]. In all cases each of the electrodes is comprised of 116 Al atoms in a face-centered cubic structure exposing (111) facets, and all the Si dangling bonds not involved in bonding with the electrodes are passivated by hydrogen.

The electronic spectrum of each of the fully hydrogen-passivated free (unattached) longer wires exhibits a fundamental energy gap between the valence and conduction states [6]. The local density of states (LDOS) for the short cluster bridge [Si_{24}NW, Fig. 2(e)] and for the bridge with the cluster doped endohedrally by an Al atom [Si_{24}AlNW, Fig. 2(f)] reveals a finite DOS in the gap both in the region of the wire bonded directly to the Al electrode (I) and the one in the middle of the cluster bridge (II). This correlates with a calculated finite electronic conductance [7] through the undoped bridge ($G \approx 0.45 g_0$, where $g_0 = 2e^2/h$) with a significant enhancement upon doping ($G \approx 1.33 g_0$).

For the longer wires, the LDOS calculated in different regions of the wires [defined in Fig. 2(g)] are shown in Figs. 2(a)–2(d). For all wires the LDOS at the interfacial regions closest to the metal electrode differ from those in the middle section of the wire, showing for the former a finite DOS in the gap indicating a metallization of these regions (see, in particular, region I), with a gradual "emptying" of the gap as a function of distance from the electrode. Convergence to the corresponding "bulk" limit (i.e., to that calculated at the middle segment of the wire) is rather fast, occurring over a range of ~5 Å [compare regions III and IV with regions I and II in Figs. 2(a) and 2(d)].

While doping is likely to be unadvisable in nanoscale systems because of expected large device-to-device statistical variation in dopant concentrations [8], the CD SiNWs offer a unique doping strategy through insertion of (interstitial) dopants into the cluster cages which are stabilized by endohedral doping. Modifications of the electronic properties of the CD Si_{96}NW wire via doping with Al atoms are illustrated in Figs. 2(b) and 2(c), respectively, for partial ($Si_{96}Al_2$NW, where only the second and fourth cages are doped) and full [$Si_{96}Al_5$NW; see Fig. 1(b)] doping. The LDOS is enhanced in the gap for regions [I and II in Figs. 2(b) and 2(c)] closest to the metal electrodes, and

 0031-9007/00/85(9)/1958(4)$15.00

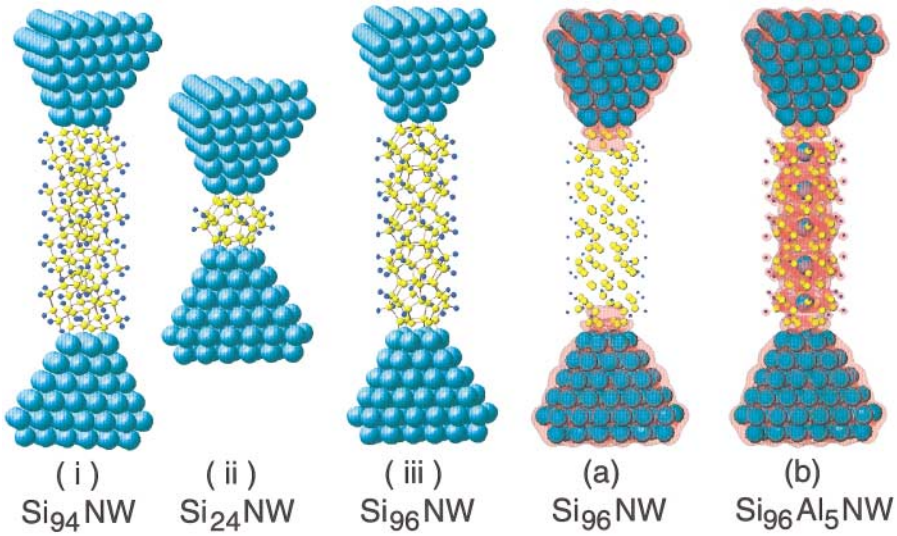

FIG. 1 (color). Passivated silicon nanowires attached to Al electrodes. The Si, H, and Al atoms are depicted as yellow, small dark blue, and larger light blue spheres, respectively. (i) Si_{94}NW etched from bulk silicon (diamond); long axis along the (211) direction. (ii) Si_{24} bridge (Si_{24}NW) and (iii) SiNW made of five Si_{24} clusters (Si_{96}NW). The lengths of the wires (measured between the interfacial Si atoms bonded to the Al electrodes at the ends) are (i) 25.305 Å, (ii) 4.98 Å, and (iii) 24.905 Å. (a),(b) Isosurfaces of the densities of states in the vicinity of the Fermi level, calculated for the cluster-derived undoped Si_{96}NW (a) and for the fully doped $Si_{96}Al_5$NW (b). The isosurfaces (pink) are superimposed on the atomic configurations of the wires.

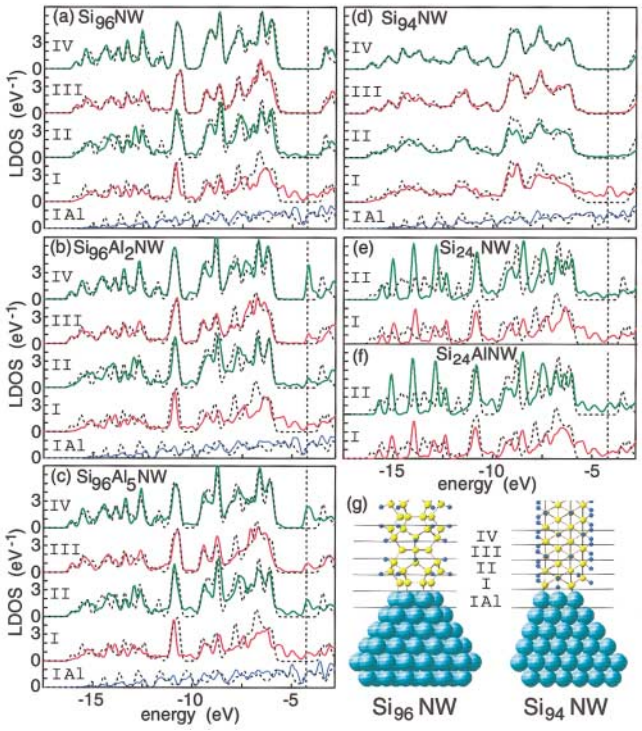

FIG. 2 (color). Local densities of state: (a)–(c) Undoped cluster-derived Si_{96}NW (a), partially doped $Si_{96}Al_2$NW (b), and fully doped $Si_{96}Al_5$NW (c); (d) diamond-structured Si_{94}NW; (e) undoped Si_{24}NW and (f) doped Si_{24}AlNW cluster bridges. In each case the LDOS is calculated in a cylinder of radius 5.73 Å about the middle axis of the wire, and the various regions are denoted in (g); the thicknesses of the SiNW regions are 2.49 Å in (a)–(c),(e),(f) and 2.2 Å in (d), and that of the Al region (IAl) is 2.34 Å. Superimposed in each case (dashed line) is the LDOS at the middle section of the corresponding fully passivated wire. The discrete spectra were broadened by a Gaussian of 0.1 eV width. The vertical dashed line denotes E_F and the vacuum energy is at $E = 0$.

the gap shrinks gradually in interior regions (e.g., regions III and IV) as the number of dopants increases [compare region IV in Figs. 2(a)–2(c)]. In both of the Al-doped wires E_F straddles the bottom of the conduction states manifold.

Analysis of the charge density ρ_{gap} corresponding to states with energies in the gap region shows that these MIGS [9–11] extend into the metal but decay rapidly into the SiNW [12]. Consequently, while for the short undoped (as well as doped) Si_{24}NW ρ_{gap} bridges the two metal electrodes, this is not the case for the longer undoped nanowires [see, e.g., Fig. 1(a)]. However, in the doped CD wires ($Si_{96}Al_2$NW and $Si_{96}Al_5$NW) ρ_{gap} extends across the entire length of the nanowire [see, e.g., Fig. 1(b)]. Inspection of the charge density difference between the electrode-attached SiNWs and their separated components (i.e., end-unpassivated wires and bare Al electrodes) shows the occurrence of charge transfer ($\sim 0.3e$) from the metal into the semiconductor, highly localized at the region of contact between them and resulting in interfacial dipoles of ~ 2 debye [13].

From the position of E_F in the electrode-attached wires and the position (E_c) of the bottom of the conduction states in the middle section (bulk) of the wire we calculate the following Schottky barrier (SB) heights: $V_{SB}(Si_{96}NW) = 0.9 \pm 0.05$ eV and $V_{SB}(Si_{94}NW) = 1.2 \pm 0.05$ eV. These values exhibit a dependence on the type of SiNW and on the atomic structure of the nanowire-to-metal interface, and they are larger by 40% to 90% than the Schottky barrier height at the bulk contact between silicon and aluminum [10,11,14]. Further analysis shows strong pinning of the nanocontact Fermi energy at the nanowire neutrality level [15]. These results could not have been anticipated or extrapolated from prior studies of bulk interfaces [9–11,14] because of the reduced dimensions of our systems; note, in particular, the much wider energy gap (~ 2.5 eV) considered here [6] which could have been expected [9] to strongly decrease the penetration depth [12] of the MIGS, the discrete nature of the nanowire spectrum (in particular, interfacial gap states)

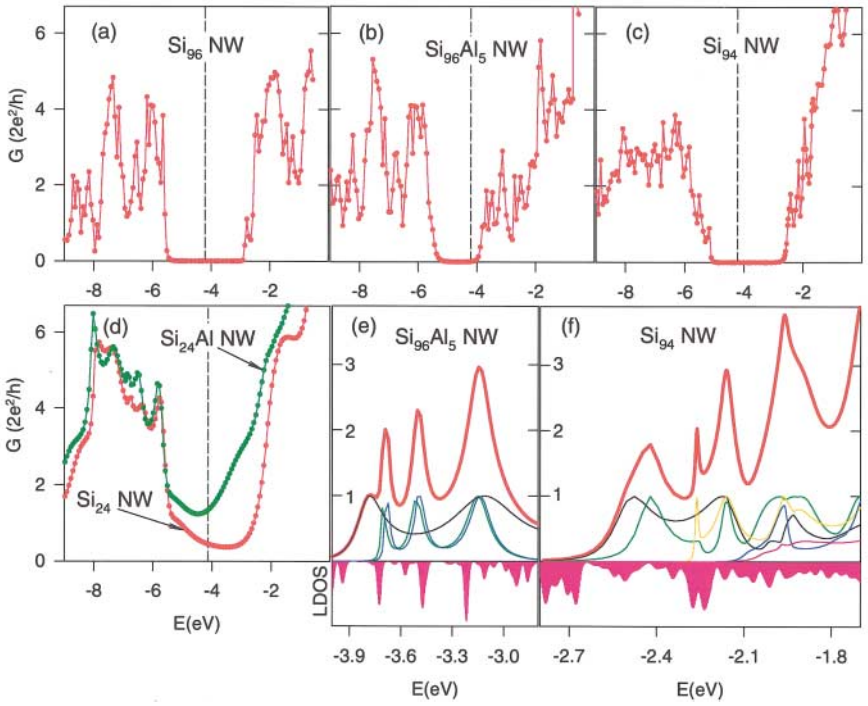

FIG. 3 (color). (a)–(d) Total conductance spectra of CD Si_{96}NW (a), CD $Si_{96}Al_5$NW (b), DS Si_{94}NW (c), and the silicon bridges [(d), where the results for Si_{24}NW and Si_{24}AlNW are depicted in red and green, respectively]. The vertical dashed line denotes E_F and the vacuum level is at $E = 0$. (e),(f) Expanded view of the total conductance (G, heavy red line) and the contributions from individual eigenchannels (in each case up to the first five channels, separated by color) for $Si_{96}Al_5$NW (e) and Si_{94}NW (f). At the bottom of (e),(f) we display the LDOS calculated at the middle of the corresponding wire. In all cases, the contribution from direct tunneling between the Al electrodes is insignificant. G is in units of $2e^2/h$, energy is in eV, and LDOS is in arbitrary units.

which could have influenced the degree of pinning in the nanocontact, and the small (finite) lateral dimensions of the interfacial dipoles [13] and their influence on the energetics of the nanoscale Schottky barrier.

The calculated conductances [7] of the nanowires versus energy are displayed in Fig. 3. These energies may be accessed through the application of a gate voltage V_G. The conductances portray overall the global shape of the corresponding LDOS (Fig. 2), with a finite conductance at E_F (i.e., at $V_G = 0$) found only for the undoped and doped Si_{24}NW bridges [Fig. 3(d)]. Additionally, doping significantly reduces the conductance threshold energy E_{th} (i.e., the energy interval between E_F and the onset of finite conductance) for transport through the conduction states [compare Fig. 3(b) with Fig. 3(a)].

A prominent characteristic of the calculated conductance is the occurrence of conductance spikes, particularly for the longer CD and DS nanowires. The conductance spectra reveal that together with DOS effects their variations with energy are punctuated by the opening of new conductance channels, modulated by the energy dependence of the transmission probabilities of the channels, as well as by interference effects. This can be seen from expanded views near the conduction-manifold threshold regions for the CD $Si_{96}Al_5$NW and DS Si_{94}NW nanowires shown in Figs. 3(e) and 3(f), respectively, where in addition to the total conductance we display the contributions to the conductance from individual eigenchannels [7]. For the CD $Si_{96}Al_5$NW [Fig. 3(e)] we note the simultaneous opening, at $E = -3.75$ eV, of two quasidegenerate channels, reflecting the approximate axial cylindrical symmetry of the wire [16]. After opening of a conductance channel its transmission rises to about unity and exhibits subsequently fluctuations between maximal values (close to unity in most cases) originating from interference resonances, as the eigenchannels scatter from the two ends (contacts) of the wire [17]. Indeed, comparison of the LDOS spectra given at the bottom of Figs. 3(e) and 3(f) with the total conductance spectra shows that the structure of the latter does not always follow that of the former. For example, focusing on the high conductance (fourth) peak at -2 eV in Fig. 3(f), we find that it does not correlate directly with a strong LDOS feature; instead, it is the result of interference resonances, with contributions from up to six different conductance eigenchannels.

The research at Georgia Tech is supported by U.S. DOE Grant No. FG05-86ER-45234. We thank A. Canning for assistance in parallelizing the computer code and K. Satler for a useful conversation. Calculations were performed on an IBM SP2 parallel computer at the Georgia Tech Center for Computational Materials Science.

[1] See special issue on "Nanometer Scale Science and Technology" [Proc. IEEE **85**, No. 4 (1997)].

[2] We used the local density-functional (LDA) method with nonlocal pseudopotentials [N. Troulier and J. L. Martins, Phys. Rev. B **43**, 1993 (1991)] and a plane-wave basis with a cutoff energy of 274 eV. For details of the method where no periodic replications or a supercell is used, see R. N. Barnett and U. Landman, Phys. Rev. B **48**, 2081 (1993). All the wires were fully relaxed. Previous calculations were limited to band structures of infinite unrelaxed wires using semiempirical pseudopotentials [C.-Y. Yeh, S. B. Zhang, and A. Zunger, Phys. Rev. B **50**, 14 405 (1994)] and to unrelaxed chains of up to eight Si atoms with jellium substrates using LDA with local pseudopotentials [J.-L. Mozos *et al.,* Phys. Rev. B **56**, R4351 (1997)].

[3] (a) H. Namatsu *et al.,* J. Vac. Sci. Technol. B **15**, 1688 (1997); (b) K. Morimoto *et al.,* Jpn. J. Appl. Phys. **35**, 853 (1996); (c) Y. Nakajima *et al., ibid.* **34**, 1309 (1995); (d) N. Wang *et al.,* Phys. Rev. B **58**, R16 024 (1998); S. T. Lee *et al.,* MRS Bull. **24**, 36 (1999); (e) A. M. Morales and C. M. Lieber, Science **279**, 208 (1998).

[4] The Si_{24} building block for the SiNWs is a "fullerene"-like cage with two opposing hexagonal rings connected by 12 pentagons. The hexagons define an inequivalent growth axis. In the relaxed hydrogen-passivated Si_{24} cluster the bonding angles are close to the ideal tetrahedral angle.

[5] The bonding geometry at the contact between the cluster-derived SiNW and the (111) top facet of the Al electrode was determined through optimization of the bonding configuration of Si_{24} on Al(111) with all the Si dangling bonds passivated by hydrogens except for the six interfacial Si atoms bonded directly to the metal. The distance between the interfacial Si and Al layers is $d(\text{Al-Si}) = 2.47$ Å. For the diamond-structured Si_{94}NW [Fig. 1(i)] the contact geometry was determined via comparison of the total energies for several judiciously chosen relaxed bonding arrangements [$d(\text{Al-Si}) = 2.38$ Å].

[6] For the fully passivated free Si_{96}NW and Si_{94}NW the gaps are 2.42 eV and 2.52 eV, respectively, in agreement with bulk LDA calculations [D. M. Bylander and L. Kleinman, Phys. Rev. B **54**, 7891 (1996)]; the gaps at the middle of these two wires when attached to the aluminum electrodes are 2.51 eV and 2.57 eV, respectively, indicating that they are sufficiently long to achieve the "bulk limit" in the mid-sections, despite their reduced lateral dimensions. Because of the lack of translational periodicity, here and in our analysis of Schottky barriers and transport properties, only the fundamental gap enters, while for bulk silicon/metal interfaces it is the much smaller ($\sim$1.1 eV) indirect gap which is considered [10,11,14].

[7] In conductance calculations we followed K. Hirose and M. Tsukada, Phys. Rev. B **51**, 5278 (1995) in conjunction with the self-consistent effective potentials calculated for the geometries shown in Fig. 1 (as well as for the Al-doped wires), using LDA with local pseudopotentials for the Si (see Ref. [11], Table I, $V_{\text{ion}}^{\text{Si}}$), the Al [L. Goodwin *et al.,* J. Phys. Condens. Matter **2**, 351 (1990)], and the H (see Ref. [2]) atoms. We used 512 plane waves to assure convergence. Transformation to nonmixing eigenchannels was performed following M. Brandbyge *et al.,* Phys. Rev. B **56**, 14 956 (1997). The total conductance is expressed as $G = g_0 \sum_n |\tau_n|^2$, where $0 \leq |\tau_n|^2 \leq 1$ is the transmission probability of the nth eigenchannel.

[8] F. G. Pikus and K. K. Likharev, Appl. Phys. Lett. **71**, 3661 (1997).

[9] V. Heine, Phys. Rev. **138**, A1689 (1965).

[10] J. Tersoff, Phys. Rev. Lett. **52**, 465 (1984).

[11] S. G. Louie and M. Cohen, Phys. Rev. B **13**, 2461 (1976).

[12] Defining the penetration depth δ as $\overline{\rho}_{\text{gap}}(z = \delta)/\overline{\rho}_{\text{gap}}(z_0) = 1/e$, where $\overline{\rho}_{\text{gap}}(z)$ is the laterally averaged charge density with z_0 at the midpoint between the interfacing Al and Si layers gives $\delta = 3.2$ Å and 2.6 Å for Si_{96}NW and Si_{94}NW, respectively, correlating with the highly localized nature of the interfacial dipoles and comparable to the value at a macroscopic Al/Si interface [11].

[13] These highly localized interfacial dipoles are of nanoscale lateral dimensions and their potential decreases with distance along the nanowire axis, unlike the case of bulk interfaces where a laterally infinite interfacial dipole layer is formed with a constant potential outside the dipole layer.

[14] E. H. Rhoderick and R. H. Williams, *Metal Semiconductor Contacts* (Clarendon, Oxford, 1988), Chap. 2.

[15] In the Schottky model [14] $V_{\text{SB}}^{S} = E_c - \varphi_m$, where φ_m is the metal work function. For φ_m and E_c calculated for the *separated* Al electrode and fully passivated Si nanowire $V_{\text{SB}}^{S}(\text{Si}_{96}\text{NW}) = 0.65$ eV and $V_{\text{SB}}^{S}(\text{Si}_{94}\text{NW}) = 1.0$ eV, which clearly underestimate the values predicted from our full calculations. Alternatively, in the Bardeen limit [14] $V_{\text{SB}}^{B} = E_c - \varphi_0$, with φ_0 the neutrality level of the free (unpassivated) semiconductor surface. Calculating φ_0 as the "center of gravity" of the density of the surface states of the (separated) Si nanowires (with their end facets unpassivated) yields φ_0 (Si_{96}NW) = 1.63 eV and φ_0 (Si_{94}NW) = 1.35 eV, measured with reference to the top of the valence states. With the energy gaps of the unattached wires [E_g (Si_{96}NW) = 2.50 eV and E_g (Si_{94}NW) = 2.76 eV] we obtain $V_{\text{SB}}^{B}(\text{Si}_{96}\text{NW}) = 0.87$ eV and $V_{\text{SB}}^{B}(\text{Si}_{94}\text{NW}) = 1.32$ eV, which are close to the values obtained from our full calculations, implying that the location of the neutrality level (with respect to E_c) is only weakly perturbed upon nanocontact formation and that the density of interface states is sufficiently high for strong pinning of E_{F} at the nanocontact neutrality level.

[16] E. N. Bogachek *et al.,* Phys. Rev. B **56**, 1065 (1997).

[17] The energy separation between such transmission "transparencies," resulting from constructive interference (Ramsauer-Townsend resonances), is proportional to $1/L^2$, where L is the effective length of the wire [E. Merzbacher, *Quantum Mechanics* (Wiley, New York, 1961)]. Indeed, such resonances in the short bridge [Fig. 3(d)] are much more widely spaced than in the longer wires.